

Determination of In Vivo Three-Dimensional Lower Limb Kinematics for Simulation of High-Flexion Squats

P.D. Wong¹, B. Callewaert², K. Desloovere², L. Labey¹, and B. Innocenti¹

¹ European Centre for Knee Research, Smith & Nephew, Leuven, Belgium

² University Hospital Pellenberg, Katholieke Universiteit Leuven, Leuven, Belgium

Abstract—In vitro and numerical simulations of the knee require reasonable kinematic and load inputs and boundary conditions, in order to help ensure their clinical relevance. However, previous simulations of high-flexion squats often have applied loads and motions that possibly oversimplify the true knee kinematics. This study aimed to improve future simulations of squatting by obtaining three-dimensional squat kinematics from a cohort of healthy adults. Seventeen subjects (age range 24-75) underwent motion capture sessions using a standard, systematic clinical procedure. Joint positions were normalized versus femur and tibia segment lengths, and ground reaction forces were normalized versus body weight. Range of motion and velocity decreased with age. The ankle was more anterior to the hip with decreasing hip height. Dynamic squat kinematics were reported.

Keywords—squat, high flexion, motion analysis, knee simulator, healthy subjects

I. INTRODUCTION

Researchers often perform in vitro or computational studies to simulate in vivo knee biomechanics. This gives an alternative when in vivo studies are impractical or invasive to patients. The clinical relevance of these simulations then relies on the definition of plausible load inputs and boundary conditions. For example, previous studies often use electromechanical systems and computer modeling to simulate the knee joint during a squat, which requires various assumptions about motion curves, loads, and muscle connections [1,2].

Although such studies have produced much useful information so far, their clinical relevance still may be limited. The squat kinematic simulators in the literature today are modeled off the “Oxford Rig” design reported in 1997 [3]. This machine advanced research capabilities at the time, as it was a controllable six-degree-of-freedom joint simulator that could produce vertical motion. However, it lacked the ability to control anteroposterior or mediolateral motion, and therefore could only simulate a simplified squat, more like squat up against a wall (Fig 1).

Better knee simulations should incorporate the full three-dimensional motions of the lower limb to be more realistic. This could hypothetically allow more accurate simulations

of joint loads, which then can better aid the evaluation of knee pathology and treatments. However, the literature lacks attempts to define “average” or standard squat kinematics. Without this data, the design of better test systems is based more on assumption rather than a population.

Considering this problem, this study attempted to define three-dimensional lower-body kinematics of typical adult subjects while they performed high-flexion body-weight squats. It would normalize the data and report it in a general form that can act as inputs to knee kinematics simulations, particularly for electromechanical machines that are more complex than the first Oxford Rig.

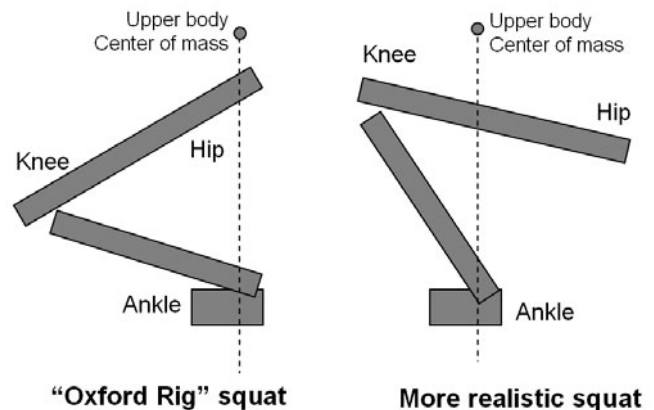


Fig. 1 Schematic lateral view of a simulated deep squat where the hip lies directly over the ankle, versus more realistic squat kinematics

II. MATERIALS AND METHODS

Seventeen adult subjects (age range 24-75, 6 female, 11 male) with no reported musculoskeletal pathologies volunteered for this study after giving informed consent. They each underwent one motion analysis session, using a 14-camera optical motion tracking system (Vicon, Oxford, UK), two forceplates (AMTI, Watertown, MA, USA), and a standard clinical kinematic model (Plug-in-Gait [4] with Knee Alignment Device [5], Vicon, Oxford, UK). In each session, a subject was asked to stand with their feet over two separate forceplates, which were spaced 115mm apart, and then perform a high-flexion squat. This consisted of descending as far down as comfortably possible, and then

rising back up to standing position, without using upper limb support (e.g., no holding the thighs with the hands). Beyond these instructions, all subjects used self-selected speeds and postures. Three repeated squat trials were taken, and one trial for each subject with no loss of balance was identified for further analysis.

Subject age, height, and mass were recorded. The motion tracking system measured ground reaction forces, calculated joint centers based on skin marker trajectories, and calculated joint rotations with Euler angles. Femur and tibia segment lengths were measured from the motion tracking data with automated algorithms (Matlab, Mathworks, Natick, MA, USA). Femur length was taken as the average distance between the hip joint center and knee joint center throughout the squat, and tibia length was taken similarly between the knee and ankle. The femur-to-tibia length ratio (Fem/Tib) and total femur-plus-tibia leg length (Fem+Tib) were recorded for each subject.

Data were then generalized, so that they could be used as inputs into typical load- and motion-controlled knee simulators, which often use linear actuators. Linear translations were measured as follows (Fig 2).

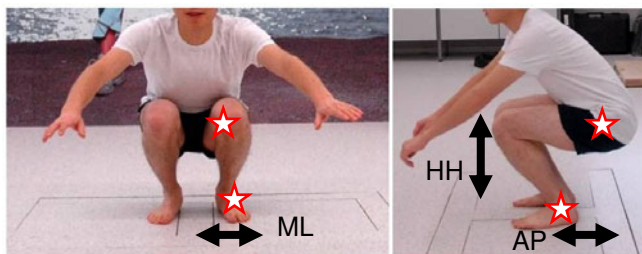


Fig. 2 Dynamic joint distances reported, between ipsilateral ankle and hip

The vertical distance between the hip and ankle joint centers was taken as hip height (HH). The distance of the ankle away from the hip was also recorded in the anteroposterior (AP) and mediolateral (ML) directions. Anterior and medial positions of the ankle gave positive values. The HH, AP, and ML directions were perpendicular and defined according to the laboratory coordinate system, since subjects faced the same direction throughout the squat. These distances were normalized by dividing them by the total Fem+Tib length. Ground reaction forces were normalized against individual body mass and expressed as N/kg. All dynamic data also were normalized in time across a 0-100% squat cycle, where the start and end points of a squat were defined at times of maximal knee extension. The normalized data were averaged using a random leg of each subject, and the resulting curves were reported. Correlations were analyzed between age and the other discrete measurements, with significance of the correlations tested with $\alpha=0.05$.

III. RESULTS

Average subject characteristics ($n=17$) are summarized in Table 1. Subjects had a healthy average body-mass index but still exhibited a wide variety of characteristics.

Table 1 Subject characteristics

	Mean	SD	Min	Max
Age (y)	49.8	15.3	23.9	75.4
Mass (kg)	71.8	13.5	45.3	97.6
Height (cm)	172.9	9.5	158.0	190.0
Body-mass index	23.9	3.8	17.7	30.8
Femur length (mm)	404.1	30.0	364.0	455.5
Tibia length (mm)	407.1	26.8	364.7	454.1
Fem+Tib (mm)	811.1	54.5	733.4	909.6
Fem/Tib ratio	0.993	0.040	0.931	1.067
Squat cycle time (s)	4.207	1.411	2.320	7.050

For each year older, squat times slowed by 0.0634 s, minimum HH increased by 0.50% of Fem+Tib length, and maximum knee flexion decreased by 0.70° ($p<0.01$) (Fig 3).

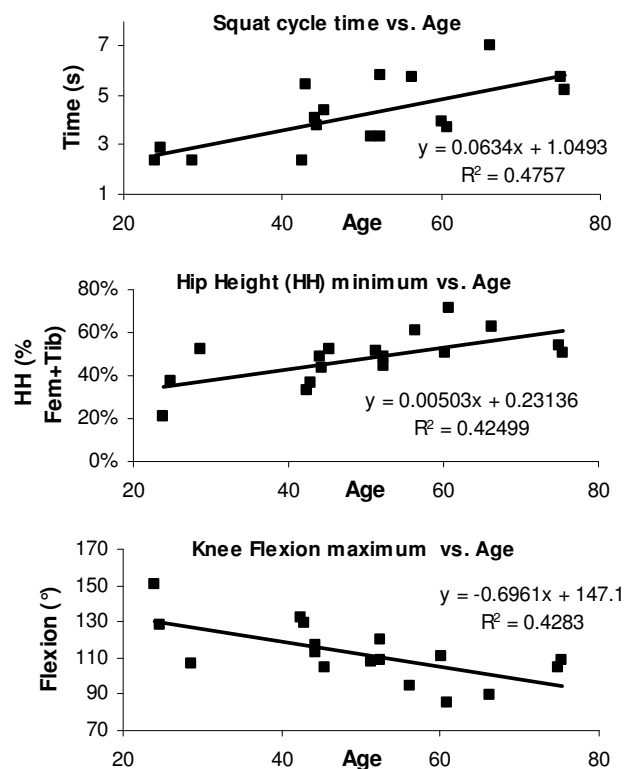


Fig. 3 Squat cycle time, HH minimum, and knee flexion maximum, for subjects. HH is expressed as a percent of the femur+tibia length.

Ground reaction forces were nearly constant during the squat, with normalized mean anterior forces of 0.014 N/kg (SD 0.028), medial forces of 0.439 N/kg (SD 0.127), and upward vertical forces of 4.90 N/kg (SD 0.234) (Fig 4).

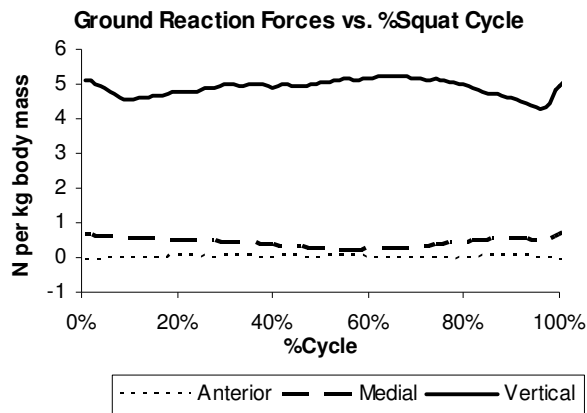


Fig. 4 Mean ground reaction forces during squats.

The average knee rotation curves in the three anatomical planes were plotted versus the squat cycle (Fig 5). Mean maximum knee flexion angle was 112.4° (SD 16.3).

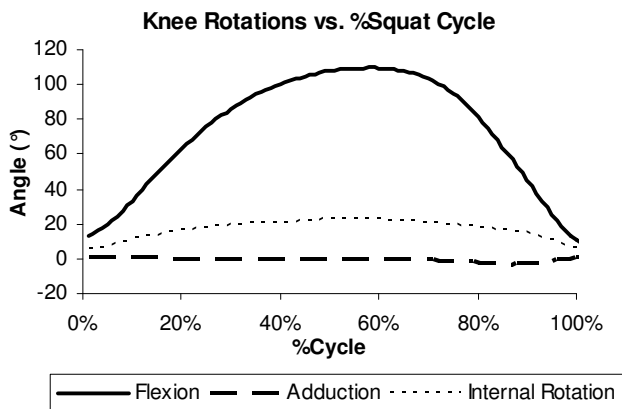


Fig. 5 Mean 3D knee rotation angles during squats.

Mean 3D distances between hip and ankle joints were plotted versus the squat cycle (Fig 6). The ML position of the ankle was nearly constant, staying lateral to the hip by 10.5% (SD 5.2) of the Fem+Tib length. The mean AP ankle position changed throughout the squat, starting and ending at 3.4% (SD 4.7) posterior to the hip and going to 21.2% (SD 5.8) anterior to the hip. The mean HH at the lowest point of the squat was 48.2% (SD 11.9).

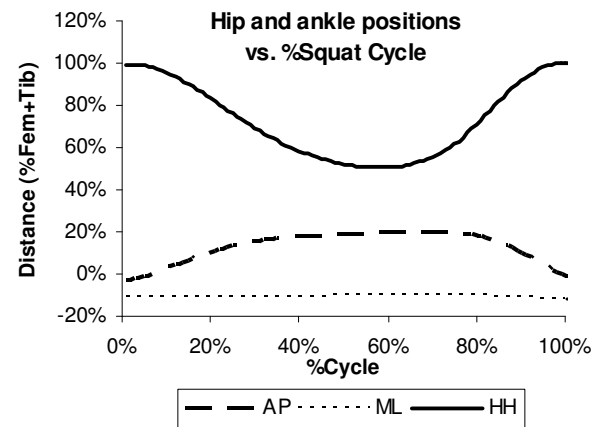


Fig. 6 Mean hip height (HH) superior to the ankle, anteroposterior distance of the ankle from the hip (AP), and mediolateral distance of the ankle from the hip (ML). Anterior and medial positions of the ankle are positive.

Mean AP was plotted versus mean HH, along with possible analytical estimates of the curve (Fig 7). A least-squares parabolic best-fit curve of the data had the equation:

$$AP = -0.904 * HH^2 + 0.971 * HH - 0.067 \quad (1)$$

An ellipse could better reflect the motion of some individual subjects, and one visual best-fit ellipse had the equation:

$$AP = 0.227 \sqrt{1 - HH^2} \quad (2)$$

Overall the ankle was more anterior with lower hip height. No subjects showed the ankle becoming more posterior in any part of descent, even for those subjects who descended past 50% hip height.

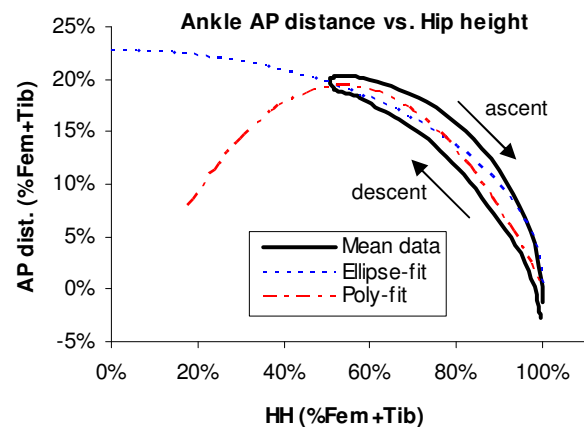


Fig 7. Mean ankle anteroposterior (AP) distance from the hip vs. hip height (HH) above ankle. Possible analytical curves to fit to the data and extrapolate to smaller HH values are shown: an ellipse and a parabola.

IV. DISCUSSION AND CONCLUSIONS

This study investigated the 3D lower-body kinematics of an unrestrained, high-flexion squat. The output data is intended to be usable as inputs into electromechanical or computational lower-body squat simulations. To do this, it analyzed healthy adults with a range of ages, anatomies, and masses. Overall patterns of hip posterior movement (or ankle anterior position) were clear with decreasing hip height. In these subjects, no relationships were found between the normalized squat kinematics and either gender or BMI, but a larger sample size could possibly show a connection. However, age was found to have significant effects. The results presented can be used to simulate the mean data of this limited cohort, but they can also be used to simulate more realistic squats of individuals with specific ages, ranges of motion, squat velocities, and bone lengths.

For example, the mean dynamic lower-body kinematics and ground reaction forces reported in Figs 4-7 can be input into a machine like that used previously by Victor et al [1], which can test cadaver specimens. Additionally, the mean curves can be adjusted according to the specimen characteristics. For example, a 90 kg donor with no musculoskeletal asymmetry would be predicted to see an ankle load under each leg with a vertical component of $90\text{kg} \times 4.90\text{N/kg} = 440\text{ N}$, or about half the body weight, based on Fig 4.

The squat range of motion and velocity can be estimated from donor age, in combination with the measurements of the femur and tibia segments. For example, using the linear best-fit equations in Fig 3, an 80-year-old donor would be predicted to squat down and back up in 6.12s, up to 91.4° knee flexion, and down to a lowest hip height above the ankle of 63.4% of the total length of the femur and tibia. The length of the undissected specimen then could be measured, from the femoral head, to the knee center, to the ankle center. All distance and time measurements can be scaled according to these values.

The dynamic kinematics curves found here can be estimated by cosine functions, if a simple analytical model is necessary, using the general equation:

$$y = \left(\frac{S - L}{2} \right) \cos\left(\frac{2\pi t}{t_{\max}}\right) + \left(\frac{S + L}{2} \right) \quad (3)$$

such that:

t = independent variable of time
 y = dependent variable to be modeled
 S = the start value
 L = the value at the lowest point of the squat
 t_{\max} = time to complete the squat cycle

Examples of this model are shown (Fig 7).

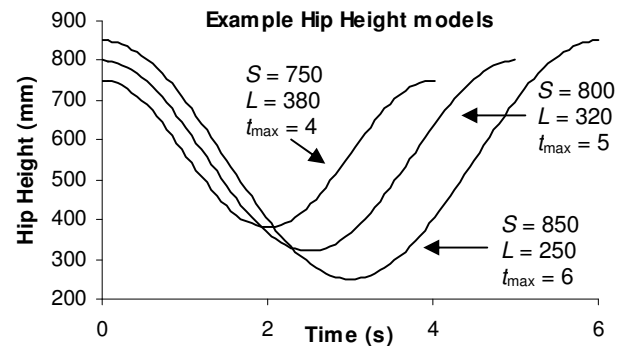


Fig 8. Example simple cosine models using Equation 3.

Individual knee simulators would customize the input curves and scales appropriately to suit their specific system requirements. Possible systems that could use these data are various mechanical test systems, finite element simulations, and numerical rigid-body simulations.

ACKNOWLEDGMENT

The authors thank Dr. Hilde Vandenuecker, Prof. Johan Bellemans, Alberto Leardini, Stanley Tsai, and the staff of Smith & Nephew for supporting for this study.

REFERENCES

1. Victor J, Labey L, Wong P et al. (2009) The influence of muscle load on tibiofemoral knee kinematics. *J Orthop Res.* Nov 4 [in press, Epub ahead of print] doi:10.1002/jor.21019
2. Baldwin MA, Clary C, Maletsky LP et al. (2009) Verification of predicted specimen-specific natural and implanted patellofemoral kinematics during simulated deep knee bend. *J Biomech.* 42(14):2341-8
3. Zavatsky AB. (1997) A kinematic-freedom analysis of a flexed-knee-stance testing rig. *J Biomech.* 30(3):277-80
4. Kadaba MP, Ramakrishnan HK, Wootten ME. (1990) Measurement of lower extremity kinematics during level walking. *J Orthop Res.* 8(3):383-92
5. Schache AG. (2006) Defining the knee joint flexion-extension axis for purposes of quantitative gait analysis: an evaluation of methods. *Gait Posture.* 24(1):100-9

Corresponding Author: Bernardo Innocenti, PhD
 Institute: European Centre for Knee Research, Smith & Nephew
 Street: Technologielaan 11 bis
 City: Leuven
 Country: Belgium
 Email: bernardo.innocenti@smith-nephew.com